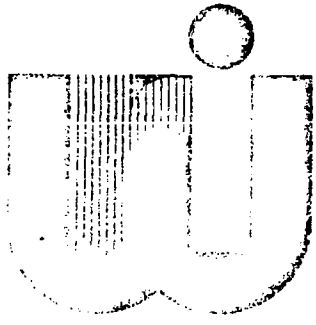

University of
Waterloo Research Institute

Numerical Simulation Studies of the Groundwater Discharge to Streams from Abandoned Uranium Mill Tailings

Final Report

June, 1984

NUMERICAL SIMULATION STUDIES OF THE GROUNDWATER DISCHARGE TO STREAMS FROM ABANDONED URANIUM MILL TAILINGS

FINAL REPORT

June, 1984

A.S. Abdul and R.W. Gillham

A RESEARCH REPORT PREPARED FOR

The National Uranium Tailings Program
Canada Centre for Mineral and Energy Technology
Energy, Mines and Resources Canada
555 Booth Street
Ottawa, Ontario
K1A 0G1

Contract No.: OSTB3-00283

File No.: 20ST.23241-3-1661

WRI Project # 310-06

Groundwater Research Institute
University of Waterloo
Waterloo, Ontario
N2L 3G1

35 pp

SUMMARY

This report presents an evaluation of the results of simulation studies of groundwater discharge to streams from abandoned uranium mill tailings and the effects of this discharge on the flux of contaminants to surface water systems. In particular, a discussion of the sensitivity of subsurface discharge to specific geometric, climatic and hydrogeologic factors is presented.

Simulations were carried out using a two-dimensional numerical finite-element unsaturated-saturated flow model. The model can account for transient boundary conditions along the atmospheric boundary and the effects of the capillary fringe on the hydraulic response of the flow system. In addition, the model describes hysteresis in the unsaturated hydraulic parameters and accounts for the compressibility of the entrapped air phase in the saturated zone.

A total of twenty-six simulations were made. The first twenty-four of these considered a tailings medium with homogeneous and isotropic hydraulic properties and with textural properties similar to those of sandy geological materials. Simulations of lateral discharges through each of four cross-sections with surface slopes of 2, 4, 8 and 16 degrees and for rainfall rates of 0.125, 0.250, 0.50, 1.0, 2.0 and 4.0 cm/hr were made. In addition, two simulations for a rainfall rate of 1 cm/hr and surface slopes of 4^{o} and 8^{o} were carried out for tailings material with hydraulic properties that are similar to those of silt-loam.

The results indicated that the actual quantity of subsurface discharge depends on many factors including rainfall rate and duration, surface slope, and texture. However, for the medium-fine sand material, subsurface discharge was always a significant component of the total discharge. Within the context of uranium tailings management this implies that large quantities of contaminants from subsurface sources of medium-textured tailings can be expected to be discharged to streams during stormflow events.

The percentage of subsurface discharge in the peak total discharge is greater at low rainfall rates and for high surface slopes, and therefore discharge from tailings with steep slopes and those experiencing low rainfall rate can be expected to have higher concentrations of contaminants than discharge from low slopes that are experiencing high rainfall rates.

Subsurface discharge through fine-textured material appears to be sluggish and to contribute insignificantly to the total discharge. Streamflow from such tailings materials will be primarily generated by rain falling on the saturated stream bed and areas adjacent to the stream. Under such conditions it can be expected that the contaminants from the shallow subsurface regions will be quickly leached out and the quality of streamflow should improve with time.

In general, typical uranium tailings are in the range of medium-to-fine grain size. Although the results in this study are very preliminary, one can speculate that streamflow from these tailings will contain a significant component of subsurface discharge. In that the pore water at shallow depths is of poor quality, there is reason to suspect that untreated runoff from such tailings will contain significant concentrations of contaminants for long periods of time.

CONTENTS

1. INTRODUCTION

1.1 Nature of the Problem

The migration of contaminants in the solution phase from uranium mill tailings can occur both by seepage through the bottom of the impoundment and by surface runoff. Both pathways must be considered in evaluating the long-term environmental effects of the tailings and in designing appropriate abandonment procedures.

Surfaces of abandoned tailings are generally traversed by a network of first-order stream channels. Streamflow is commonly intermittent, though not in all cases, and the streams may be influent or effluent, depending upon the time of year and the particular hydrogeologic setting. At sites under active management, the surface discharge is treated with barium chloride for radium removal prior to discharge to the receiving waters; however, for effective long-term management, the objective is a situation in which perpetual treatment is not required.

The mechanism of streamflow generation continues to be a controversial topic in hydrology, and one which has great bearing on tailings management. In particular, most streamflow generation mechanisms attribute the greatest proportion of flow during major runoff events to surface runoff. In contrast, tracer studies suggest that a very significant proportion of the flow, even during peak discharge, originates as groundwater. If the primary source of streamflow is surface runoff, then one would expect that within some reason-

able length of time, the readily leachable contaminants of the surface materials would be removed resulting in a gradual improvement of the runoff and streamflow quality. On the other hand, if a significant proportion of streamflow originates as groundwater, then poor-quality runoff could be expected for a very long period of time.

1.2 Previous Investigations

The capillary fringe (the zone of tension saturation above the water table), and its effects on streamflow generation and the migration of contaminants from the groundwater zone to surface waters has been under investigation at the University of Waterloo for about four years. Field, laboratory, and mathematical simulation studies have been completed or are in progress, principally through funding from Atomic Energy of Canada Ltd. (Abdul and Gillham, 1984). The results show quite conclusively, that under selected hydrogeologic conditions, the capillary fringe can result in a large groundwater contribution to streamflow. Field studies conducted in the East Arm of the Nordic tailings near Elliot Lake and at CFB Borden, Ontario, have confirmed that groundwater was a significant proportion of stormflow and that the capillary fringe was a major factor contributing to groundwater discharge in these areas, (Blowes, 1983).

A two-dimensional numerical finite-element unsaturated-saturated flow model was developed to evaluate the factors that affect the interaction of the capillary fringe and streamflow generation, while avoiding the high cost of field studies. The numerical model can account for transient boundary conditions along the atmospheric boundary and therefore can allow for the development and decay of a seepage face. In addition, the model describes hysteresis

in the unsaturated hydraulic parameters and accounts for the compressibility of the entrapped air phase in the saturated zone. Testing of the model against laboratory results and results from the literature has shown that the model can adequately simulate unsaturated-saturated flow processes and in particular, has shown that the model can adequately simulate the capillary fringe effect on streamflow generation and streamflow quality (Abdul and Gillham, 1983).

1.3 Scope and Objectives

The objective of this study was to examine the sensitivity of the components of lateral discharge to the stream to variations in such factors as; rainfall intensity, surface slope and texture of the tailings material. Only homogeneous and isotropic tailings material was to be considered. The approach taken was:

1. Select a hypothetical but realistic uranium mine tailings situation and specify a number of cross-sections for study. The cross-sections were distinguished from each other by different surface slopes.
2. Simulate the components of lateral discharge for each cross-section for a range of rainfall rates.
3. Use combinations of surface slope and rainfall intensity to simulate the lateral components of flow through tailing materials of different texture.

2. FINITE ELEMENT MODEL

The flow equation used in this study is similar to that used by Neuman, 1973 and describes unsteady flow of a slightly compressible fluid in a vertical co-ordinate system (x,z) through an unsaturated-saturated porous medium. The flow equation can be expressed as:

$$\frac{\partial}{\partial x}(KS_x Kr\ (\psi)\ \frac{\partial \psi}{\partial x}) + \frac{\partial}{\partial z}\ (KS_z\ Kr\ (\psi)\ \frac{\partial}{\partial z}\ (\psi + z)) = \frac{\partial \psi}{\partial t}\ (\gamma Ss + C\ (\psi)) \qquad (1)$$

where KS_x and KS_z are the saturated hydraulic conductivities in the x and z directions respectively, Kr is the relative hydraulic conductivity, ψ is the pressure head, z the elevation head, and γ is zero in the unsaturated zone and one in the saturated zone. Ss is the specific storage and is defined as the volume of water instantaneously released from storage per unit bulk volume of saturated soil when the pressure head is lowered by one unit. It physically represents the increase in storage that results from the combined compressibilities of the porous medium and the water it contains. The specific moisture capacity, $C(\psi)$, which is the slope of the moisture content-pressure head curve, physically represents the increase in storage that results from the actual dewatering of the pores of the porous medium. The right hand side of equation (1) represents the change in storage within the porous medium in a given interval of time, while the left hand side represents the net flux through the system during the same time period.

Important assumptions made in the development of equation (1) are:

a) flow is Darcian;

b) temperature gradients and osmotic and chemical gradients are all negligible;

c) horizontal compressibilities are small compared to vertical compressibilities of the skeleton of the porous medium;

d) the air phase in the unsaturated zone is continuous and always in connection with constant external atmospheric pressure.

In the unsaturated zone, specific moisture capacity, relative hydraulic conductivity and moisture content (θ) are functions of pressure head. As a result, these are not single-valued parameters and their dependence on ψ is described by functional relationships. This adds considerably to the difficulty in measuring and specifying the parameters, and also adds considerably to the difficulty in solving the flow equation in that it is highly nonlinear. A necessary step in developing a solution to equation (1) is the development of accurate and efficient means of representing the hydraulic parameters.

The moisture content-pressure head relationship used in this study was given by van Genuchten (1978) as

$$\theta = \theta_r + (\theta_s - \theta_r) \left\{ \frac{1}{1 + (\alpha|\psi|)^n} \right\}^m \qquad (2)$$

where θ is the volumetric water content; θs and θr are saturated and residual moisture content respectively, α and n are curve fitting parameters and $m = 1-1/n$.

Equation (2) has been extended in a previous study (Abdul and Gillham, 1983) to describe hysteresis in the $\theta(\psi)$ relationship. Rewriting equation (2);

$$\theta = (\theta_s - \theta_r)\left[\frac{1}{1 + (\alpha|\psi|)^n} \right]^m + \theta_r$$

When equation (3) is used to represent the main drying and main wetti
curves, the curve-fitting parameters are denoted by α_d, n_d, m_d and α_w, n_w a
m_w respectively and θ'r and θ's denote reversal moisture contents. To u
equation (3) to generate the primary scanning drying curves, the value of θ'
which is unique for each reversal point, is first determined. The oth
parameters in the equation are numerically equal to the values of the ma
drying curve parameters and θ'r represents the residual moisture content. T
unknown value of θ's corresponding to each reversal moisture content can
obtained from:

$$\theta_s' = \theta_r' + \frac{(\theta - \theta_r')}{\left[\frac{1}{1 + (\alpha_d|\psi|)^{n_d}}\right]^{m_d}}$$

Similarly, in applying equation (3) to describe the primary wetting scanni
curves, the unknown values for θ'r corresponding to each reversal moistu
content can be obtained from:

$$\theta_r' = \frac{\theta - \theta_s' \left[\frac{1}{1 + (\alpha_w|\psi|)^{n_w}}\right]^{m_w}}{1 - \left[\frac{1}{1 + (\alpha_w|\psi|)^{n_w}}\right]^{m_w}}$$

An expression for the specific moisture capacity, $C(\psi)$, is obtained by di
ferentiating equation (2), giving

$$C(\psi) = \frac{d\theta}{d\psi} = \frac{-\alpha n (\theta_s - \theta_r)}{(\quad)^{-m}} \; \frac{1}{S^m} \; (1 - S^{\frac{1}{m}})^n$$

where H = θ - θr/θs - θr. The hydraulic conductivity-moisture content relationship used in this study is of an exponential form (Gillham, 1976):

$$K(\theta) = \alpha\theta^{\beta} \tag{7}$$

where α and β are curve fitting parameters. By this relationship, laboratory values of $K(\theta)$ and θ should plot as a straight line on log-log paper and from such a plot the slope (β) and intercept (α) can be readily determined.

It is generally agreed that on rewetting a porous medium to 'saturation', a portion of the void space will be occupied by entrapped discrete air bubbles. Gillham (1976) has observed that entrapped air can occupy up to 10% of the volume of the porous medium. The compressibility of the air-water mixture in the saturated zone is much larger than that of water and the porous medium and therefore its effect on storage in the saturated zone can be very significant. To account for the effect on storage of the compressibility of the air-water mixture the moisture content and the specific storage terms in equation (1) are replaced by the effective moisture content and effective specific storage and these terms are described by equations (8) and (9) respectively.

$$\theta' = \theta v + S(n - \theta v)(1 - Patm/P) \tag{8}$$

$$S'_s = S(n - \theta') Patm/P^2 \tag{9}$$

where θ' = effective moisture content

S = degree of saturation

n = porosity

$Patm$ = atmospheric pressure

P = pore water pressure

S'_s = effective specific storage

The length of the seepage face is not known a priori and to account for changing boundary conditions in numerical models is very challenging. In the model used in this study the length of the seepage face is determined at the end of each time step by a systematic checking of the hydraulic condition at each node on the atmospheric boundary. Starting at the lowest location on the atmospheric boundary, where the seepage face begins to propagate, a sequential check is made of conditions at each node. Nodes on the atmospheric boundary can experience either constant head (Direchlet) or flux (Neuman) boundary conditions and these conditions can change during the development and decay of the seepage face.

If a node that was under negative pressure at the start of a time step has changed to a condition of zero or positive pressure at the end of the time step, then a change in boundary condition, from Neuman to Direchlet, is implemented. Since the depth of ponding is insignificant in this analysis, ψ is set to zero at those nodes on the atmospheric boundary that are under Direchlet condition. The change to unsaturated condition is determined when infiltration is occurring at a rate that is greater than the precipitation rate and the corresponding change in boundary condition, from Direchlet to Neuman, is implemented. The extent of the seepage face is determined by checking the constant head nodes for negative (outward) fluxes.

The numerical approach taken to quantify the components of event and pre-event water in the lateral discharge to the stream is very basic in that water that is discharging through the atmospheric boundary from the medium is considered to be pre-event water while water that fails to enter the porous medium is considered to be event water. For a comprehensive development and description of the numerical approximation and validation of the flow model

used here, the reader is referred to the AECL Report by Abdul and Gillham (1983).

3. SIMULATIONS

3.1 Introduction

The cross-section shown schematically in Figure 1 is typical of first-order streams at tailings sites in the Elliot Lake area. Each cross-section has two components, a rectangular component ABCD and a triangular component ADE. The rectangular component is 3.0 m deep and 8.0 m long and the stream is 0.3 m wide. The rectangular portion of Figure 1 was used as a base and by modifying the triangular portion ADE, four cross-sections with surface slopes of 2, 4, 8 and 16 degrees were generated. Simulations of lateral discharges through each of these four cross-sections were conducted for rainfall rates of 0.125; 0.25; 0.50; 1.0; 2.0 and 4.0 cm/hr, resulting in 24 simulations. The tailings material was assumed to have homogeneous and isotropic hydraulic properties with textural properties similar to those of sandy geologic materials.

The flow domain of Figure 1 was discretized into 2,405 triangular elements with 1,278 nodes. The spatial mesh in the initially unsaturated portion of the domain was made smaller than that in the saturated portion because of the highly sensitive nature of moisture content, hydraulic conductivity and specific moisture capacity to changes in pressure head. In this zone values for x and particularly y were not allowed to exceed 10 cm. Time increments were determined within the program and was based on the number of iterations required for a solution in the previous time step.

Two simulations for a rainfall rate of 1 cm/hr and surface slopes of 4^{o} and 8^{o} were carried out for tailings material with silt-loam hydrogeologic properties. The selection of this material proved to be difficult because such a selection depends on the availability of the unsaturated hydraulic parameters which are necessary input to the numerical model. The literature has very little of such data and specific data for uranium tailings materials is almost non-existent.

3.2 Initial and Boundary Conditions

Prior to each simulation, the water table was horizontal and coincident with the stream bed. Initially, the hydraulic head was 3.0 m throughout the cross-section and the flow system was under static hydraulic conditions. The initial pressure head values at each node within the flow domain were obtained by subtracting the elevation heads from the corresponding hydraulic heads at each node.

The right, left, and bottom boundaries of the cross-sections (Figure 1) were considered to be impermeable to flow. Throughout the simulations these boundaries were under a zero flux (Neuman) boundary condition.

The boundary conditions on the atmospheric boundary were not known a priori. Surface saturation during the precipitation event would result in some atmospheric boundary nodes switching from Neumann to Direchlet type boundaries. Similarly, a reversal in the boundary condition at some atmospheric boundary nodes would occur after the precipitation event. The boundary conditions at the atmospheric nodes were determined at the end of each time step by systematically checking the hydraulic condition at each node on this boundary.

The atmospheric boundary nodes that were under a flux boundary condition were assigned a flux that was equal to the rainfall rate during the precipitation event and zero flux after the precipitation event.

3.3 Results

3.3.1 Clean, Medium-to-Fine Sand

The moisture content-pressure head curves used to describe the medium-fine tailing materials were determined in the laboratory using a clean medium to fine sand. The main drying and main wetting curves are shown in Figure 2. A saturated hydraulic conductivity of 5×10^{-3} cm/sec and a porosity of 0.40 were used in the simulations.

Referring to the main drying curve of Figure 2, the air entry value of the porous medium is about -30 cm. In a hydrogeological context, this indicates that the medium would remain saturated for a distance of about 30 cm above the water table. With a surface slope of 2^0 the entire atmospheric boundary will be initially saturated while for a surface slope of 4^0 about 56% of the surface, the lower portion, will be initially saturated. As the surface slope increases a progressively smaller percentage of the surface material will be initially saturated for an initial water-table position that is coincident with the stream bed.

Some of the results from the 24 simulations are plotted in Figures 3 through 6. Figure 3(a) shows plots of total and subsurface discharges for a rainfall rate of 1.0 cm/hr, a rainfall duration of 30 minutes and a surface slope of 2^0. Figure 3(b) shows similar plots for the same rainfall characteristics but for a surface slope of 8^0.

The results in Figures 3(a) and 3(b) show that both the total and subsurface discharges responded immediately to the precipitation event, and that throughout most of the discharge period, subsurface discharge was the main component of the lateral discharge hydrograph. In increasing the surface slope by a factor of 2 from 4^{o} to 8^{o}, the total discharge and the subsurface discharge components decreased from 10.0 and 5.5 cm^3/min to 4.5 and 3.5 cm^3/min respectively at the time of peak discharge. At peak discharge, subsurface discharge made up 78% and 55% of the total discharge for the 8^{o} and 4^{o} slopes respectively.

To irterpret the results of Figures 3(a) and 3(b) one needs to examine the initial conditions of the surface materials. Prior to the rainfall event, about 56% and 28% of the surface slope was saturated but under negative pressure for the 4^{o} and 8^{o} slopes respectively. The rapid generation of large quantities of total and subsurface discharge can therefore be explained by the initial near-stream capillary-fringe zone being rapidly converted to a positive pressure zone resulting in the rapid subsurface discharge of pre-event water to the stream.

The larger total and subsurface discharges for the 4^{o} slope as compared to the 8^{o} slope can be explained by the larger initial extent of surface saturation for the 4^{o} slope. In contrast, the larger percentage of subsurface discharge in the peak discharge from the 8^{o} slope as compared to the 4^{o} slope is due to the larger slope providing a stronger hydraulic gradient toward the stream.

The results from all 24 simulations were used to construct Figure 4 which shows plots of subsurface discharge (% of peak discharge) versus rainfall rate for the four surface slopes and a rainfall duration of 30 minutes.

Figure 4 shows that at very low rainfall rates (.125 cm/hr) and for the geologic domain being considered, total discharge is almost completely made up of subsurface discharge and that the percent of subsurface discharge in the peak total discharge is not sensitive to changes in surface slope. As the rainfall rate increases there is a general trend of increasing percent of subsurface discharge with increasing surface slope. The results indicate that a high percentage of subsurface discharge in the peak total discharge is favoured at low rainfall rates and high surface slopes.

Figure 5 shows plots of peak total discharge versus rainfall rates for the four surface slopes and a rainfall duration of 30 minutes. The results reflect the effect of the initial degree of storage within the system on the total discharge within the duration of the rainfall event. The 2^0 slope represents the limiting case, where the entire surface was initially saturated and peak discharge was linearly related to rainfall rate. For the 4^0 surface slope there was initially some storage capacity within the flow system and as such, peak discharge did not become linear with rainfall rate until the rainfall rate increased to 2.0 cm/hr. The results indicate that for the same initial conditions and rainfall duration, the peak total discharge decreases with increasing surface slope as a result of the associated increase in storage capacity of the medium.

Plots of peak subsurface discharge versus rainfall rate are shown in Figure 6 for the four surface slopes and rainfall duration of 30 minutes. The results show that as long as the flow system remains transient, peak subsurface discharge increases with decreasing surface slope. Figure 6 shows that as the rainfall rate increases, the lowest slope (2^0) was the first to reach steady state conditions. Prior to the steady state condition the system with

the 2^{o} slope had the highest peak subsurface discharge, and at higher rainfall rates the system with the 4^{o} slope had the highest peak subsurface discharge.

These results suggest that the actual magnitude of subsurface discharge is determined by both the hydraulic gradient, and the lateral extent of the seepage face. Because of the greater extent of surface saturation for the lower slopes, they would have longer seepage faces and therefore at low rainfall rates they would generate higher peak subsurface discharge than the higher slopes. However, as rainfall rates are increased, the systems with the lower slopes will reach steady state conditions and at the same time systems with steeper slopes will be developing longer seepage faces and stronger hydraulic gradients directed towards the seepage face. It seems therefore that in transient systems the peak subsurface discharge is limited by the lateral extent of the seepage face while in steady state systems the hydraulic gradient (surface slope) determines the peak subsurface discharge.

The results of Figures 4 and 6 show that although the percent of peak subsurface discharge in the peak discharge is favoured from high surface slope and for low rainfall rate, this does not necessarily mean that the peak subsurface discharge is favoured by the same combination of surface slope and rainfall rate.

3.3.2 Silt Loam Geologic Material

The moisture content-pressure head curves and the hydraulic conductivity-moisture content relationship for the silt loam is shown in Figures 7a and b, respectively. These hydraulic parameters were obtained from Mualem, 1976. Although the parameters were determined from measured data, the extremely rapid decline in hydraulic conductivity with decreasing water content (Figure 7b) is not physically reasonable. Nevertheless, for the purposes of this study,

Figures 7(a) and 7(b) were used to represent the hydraulic properties of the medium in the simulations.

Two simulations for a rainfall rate of 1 cm/hr and surface slopes of 4^{o} and 8^{o} were conducted for the silt-loam material. The geometry of the porous medium and the initial and boundary condition for these two simulations were similar to those used in the simulations for sandy materials.

The $\theta(\psi)$ relationship for the silt loam is quite different from that for the medium-fine sand in that there is a more gradual decrease in moisture content with negative pressure head for the main drying curve and a slower increase in pressure head with increasing moisture for the low pressure head range of the main wetting curve. Although the capillary fringe extended for about 20 cm above the water table, the medium was almost saturated for about 100 cm above the water table. A major difference between the medium-fine material and the silt-loam material is that the silt-loam material has a saturated hydraulic conductivity that is over an order of magnitude lower ($3x10^{-4}$ cm/sec) than that of the medium-fine material ($5x10^{-3}$ cm/sec), and, as noted above,, the hydraulic conductivity of the silt loam decreases rapidly with decreasing moisture content.

The total discharge and subsurface discharge for the two simulations are plotted in Figure 8a and b. The results show that total discharge responded rapidly to the precipitation event and reached a maximum at the time the precipitation event stopped. Further, the rate and magnitude of the response of total discharge is similar to that of the medium-fine sand material with the total discharge from the 8^{o} slope being lower than that from the 4^{o} slope. In contrast however, subsurface discharge responded very sluggishly and was always an insignificant component of the total discharge. The conversion of

the capillary fringe to a positive pressure zone did result in a rapid water-table rise and for the 4^{o} slope the water table intersected more than 50% of the ground surface at the time of peak discharge. However, because of the low hydraulic conductivity (K_s = $3x10^{-4}$ cm/sec) the hydraulic gradient was too small to cause significant discharge through the 4^{o} and 8^{o} slopes and the total discharge was generated by rain falling on the saturated surface of the stream bed and upslope of the stream.

4. DISCUSSION

The simulation results from the medium-fine sand are consistent with the results from the laboratory and field experiments conducted previously (Abdul and Gillham, (1984). The field experiments were conducted at CFB Borden, Ontario, in medium-fine sand and at the Nordic Main, West Arm, Uranium Tailings site. The results show that, under shallow-water-table conditions, the capillary fringe caused a rapid and large response in the near stream water table and this response led to the rapid generation of large quantities of subsurface and total discharges.

The results of this investigation indicate that the actual quantity of subsurface discharge depends on many factors including rainfall rate and duration, surface slope, and texture. However, for the medium-fine sand material, subsurface discharge was always a significant component of the total discharge. Within the context of uranium-tailings management, this implies that large quantities of contaminants from subsurface sources of medium-textured tailings can be expected to be discharged to streams during stormflow events.

The percentage of subsurface discharge in the peak total discharge is greater at low rainfall rates and for high surface slopes, and therefore discharge from tailings with steep slopes and those experiencing low rainfall rate can be expected to have higher concentrations of contaminants than discharge from low slopes that are experiencing high rainfall rate.

Subsurface discharge through fine textured tailing material appears to be sluggish and to contribute insignificantly to the total discharge. Streamflow from such tailing material will be primarily generated by rain falling on the saturated stream bed and areas adjacent to the stream. Under such conditions it can be expected that the contaminants from the shallow subsurface regions will be quickly leached out and the quality of streamflow should improve with time.

The predictions of this study depend strongly on the $\theta(\psi)$ and $K(\theta)$ relationships. This data is almost non-existent for uranium tailings and their measurement requires difficult and time consuming procedures. The need to develop an adequate data base for $\theta(\psi)$ and $K(\theta)$ for a range of uranium tailings material cannot be over-emphasized.

In general, typical uranium tailings are in the range of medium-to-fine grain size. Although the results in this study are very preliminary, one can speculate that streamflow from these tailings will contain a significant component of subsurface discharge. In that the pore water at shallow depths is of poor quality, there is reason to suspect that untreated runoff from such tailings will contain significant concentrations of contaminants for long periods of time. The ultimate environmental effects will of course depend significantly upon the physical and chemical processes that occur in the receiving waters. Should the potential effects be considered unacceptable, there would be two choices of remedial action. The first would involve the long-term treatment of surface waters discharged from the tailings, while the second choice would involve the development of surface designs that would minimize the discharge of pore water to the surface.

5. RECOMMENDATIONS

1. Many aspects of streamflow generation from uranium tailings sites could not be addressed in this phase of the study primarily because of the short duration of the study and the inadequate data base for the unsaturated hydraulic parameters of tailings. A logical extension of the present work should include the determination of the $\theta(\psi)$ and $K(\theta)$ relationships for uranium tailings over a wide range of texture.
2. Using the data from (1) additional simulations similar to those of the present work should be conducted.
3. The findings from the numerical simulations should be examined under field conditions.
   a. Selected tailings sites with contrasting geometric and hydrogeologic properties should be instrumented and monitored to evaluate the significance of contaminant discharge from subsurface sources to surface water.
   b. The two-dimensional flow model should be extended to a flow and transport model. Such an extension will provide a tool to evaluate the sensitivity of contaminant discharge from subsurface sources to surface waters under a range of geometric, climatic and hydrogeologic conditions.

6. REFERENCES

1. Abdul, A.S. and Gillham, R.W. Laboratory studies of the effects of the capillary fringe on streamflow generation, Water Resour. Res., 1984 (in press).
2. Abdul, A.S. and Gillham, R.W. Field investigation of the effects of the capillary fringe on streamflow generation, Water Resour. Res., 1984 (in submittal).
3. Abdul, A.S., Gillham, R.W. and Frind, E.O. Significance of the capillary fringe effect on streamflow generation and runoff quality, Final Report, Atomic Energy of Canada Ltd., Chalk River Nuclear Laboratories, Chalk River, Ontario, June 1983.
4. Blowes, D. The influence of the capillary fringe on the quantity and quality of runoff in an inactive Uranium Mill Tailings Impoundment. M.Sc. Thesis, Dept. of Earth Sciences, University of Waterloo, 1983.
5. Mualem, Y. A catalogue of the hydraulic properties of unsaturated soils, U.S.-Israel Binational Science Foundation, Research Project 442, Haifa, Israel, 1976.
6. Neuman, S.P. Saturated-unsaturated seepage by finite elements. Journal of the Hydraulics Division, A.S.C.E., HY 12, 2233-2250, 1973.

ACKNOWLEDGEMENTS

The authors wish to thank Ray Carter for his assistance in preparing this report, Marilyn Bisgould for typing this manuscript, and Nadia Bahar for doing the drafting.

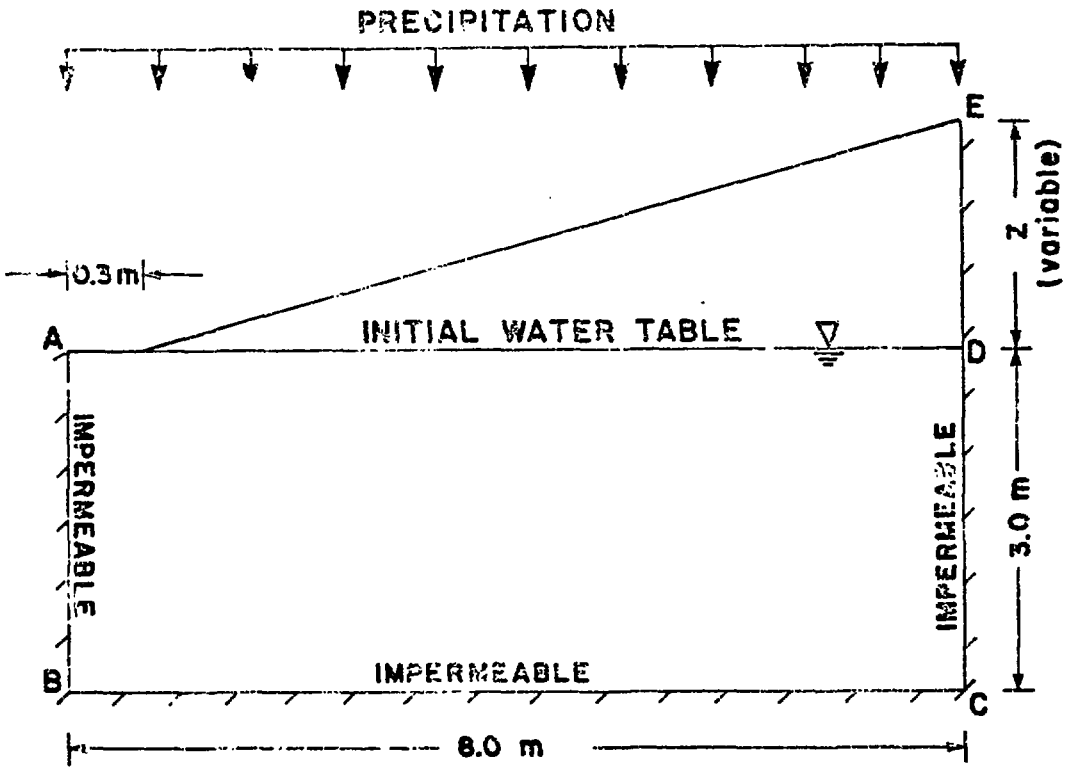

Figure 1. Hypothetical cross-section

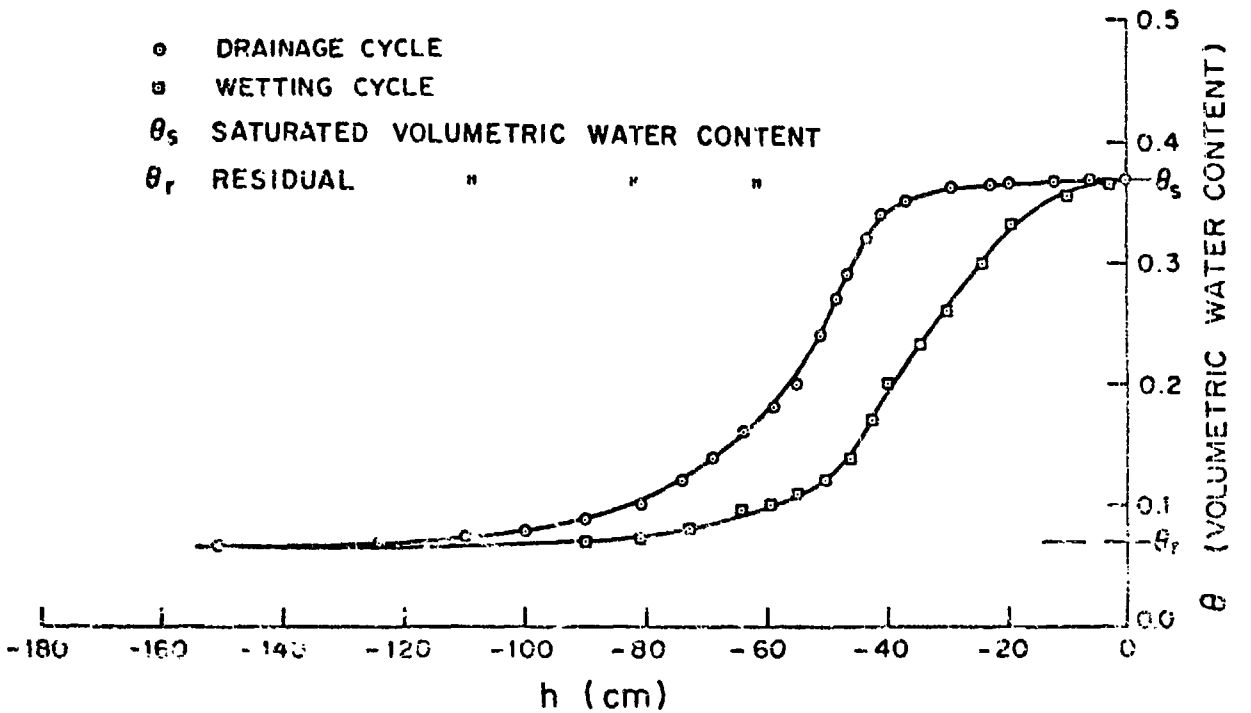

Figure 2. Wetting and drainage curves for medium-fine sand

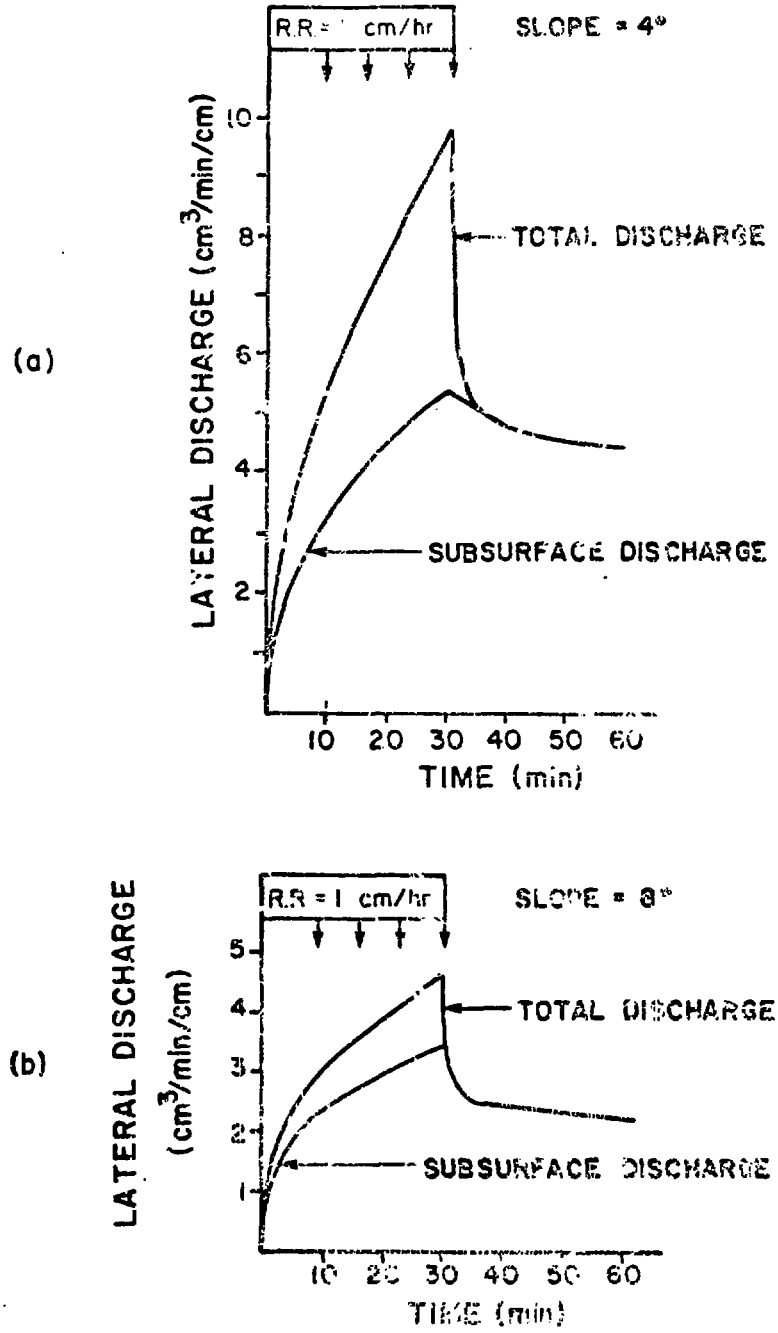

Figure 3. Hydrographs for medium-fine sand: (a) surface slope = 4°
(b) surface slope = 8°

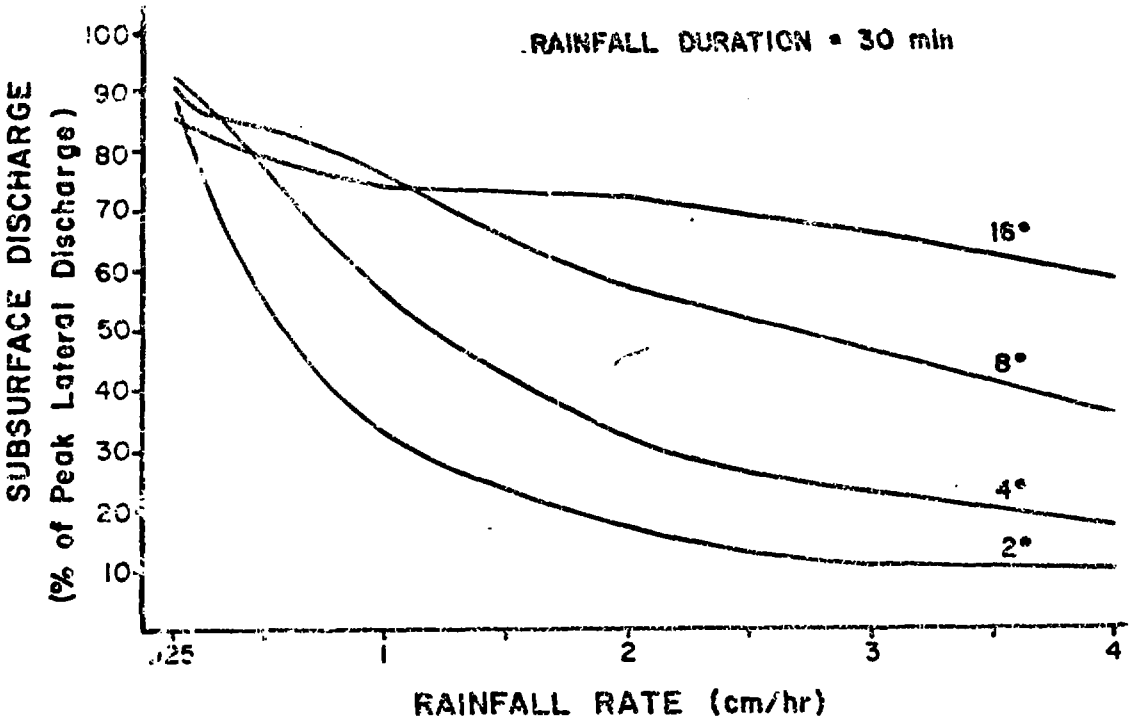

Figure 4 Percentage subsurface discharge versus rainfall rate for various surface slopes

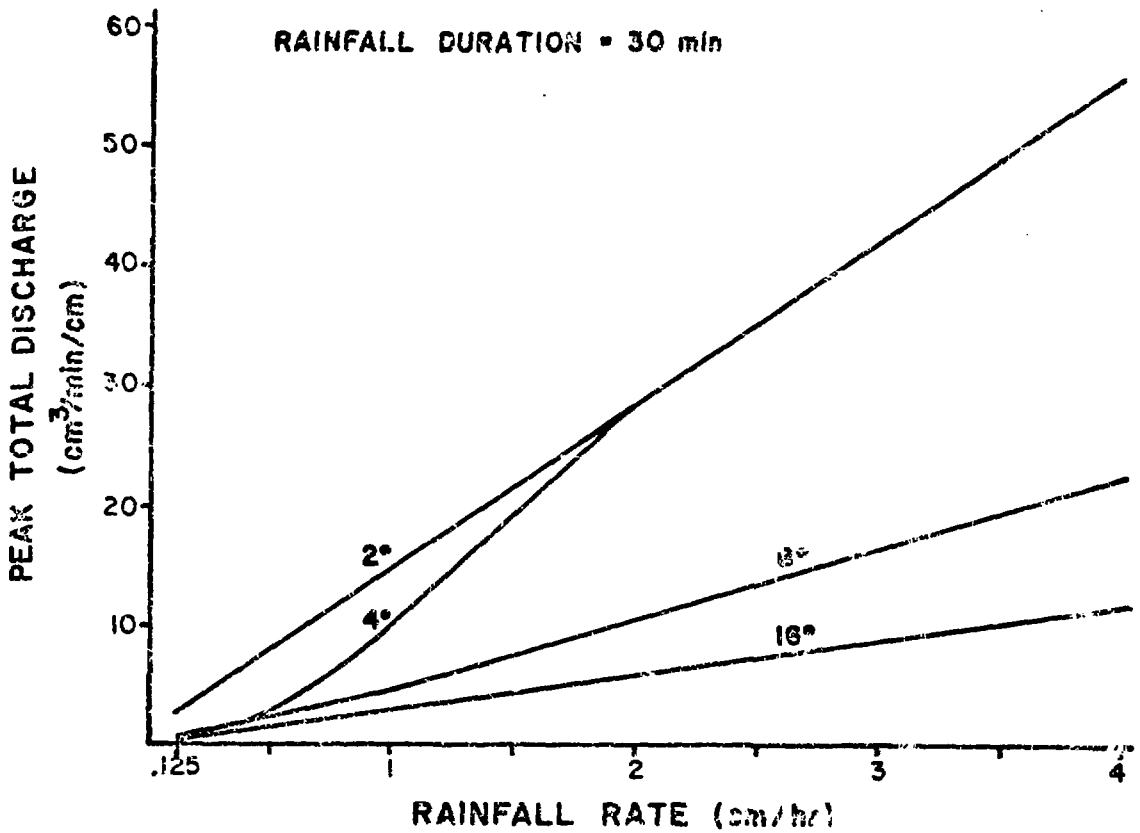

Figure 5. Peak total discharge versus rainfall rate for various surface slopes

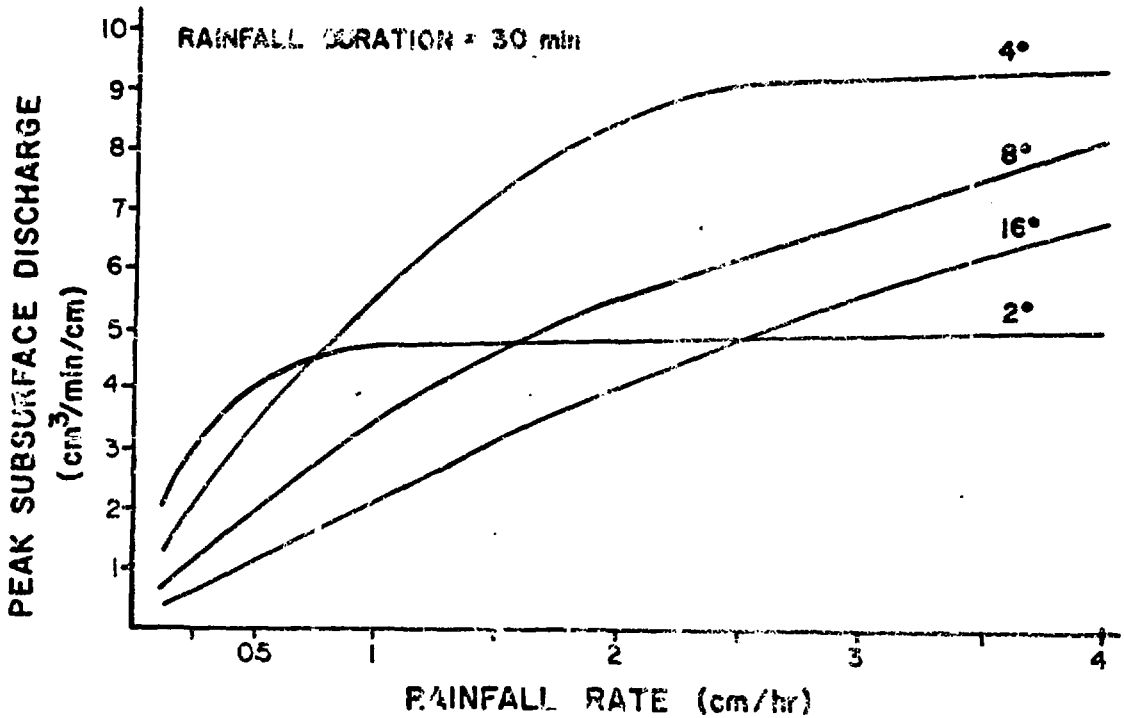

Figure 6. Peak subsurface discharge versus rainfall rate for various surface slopes

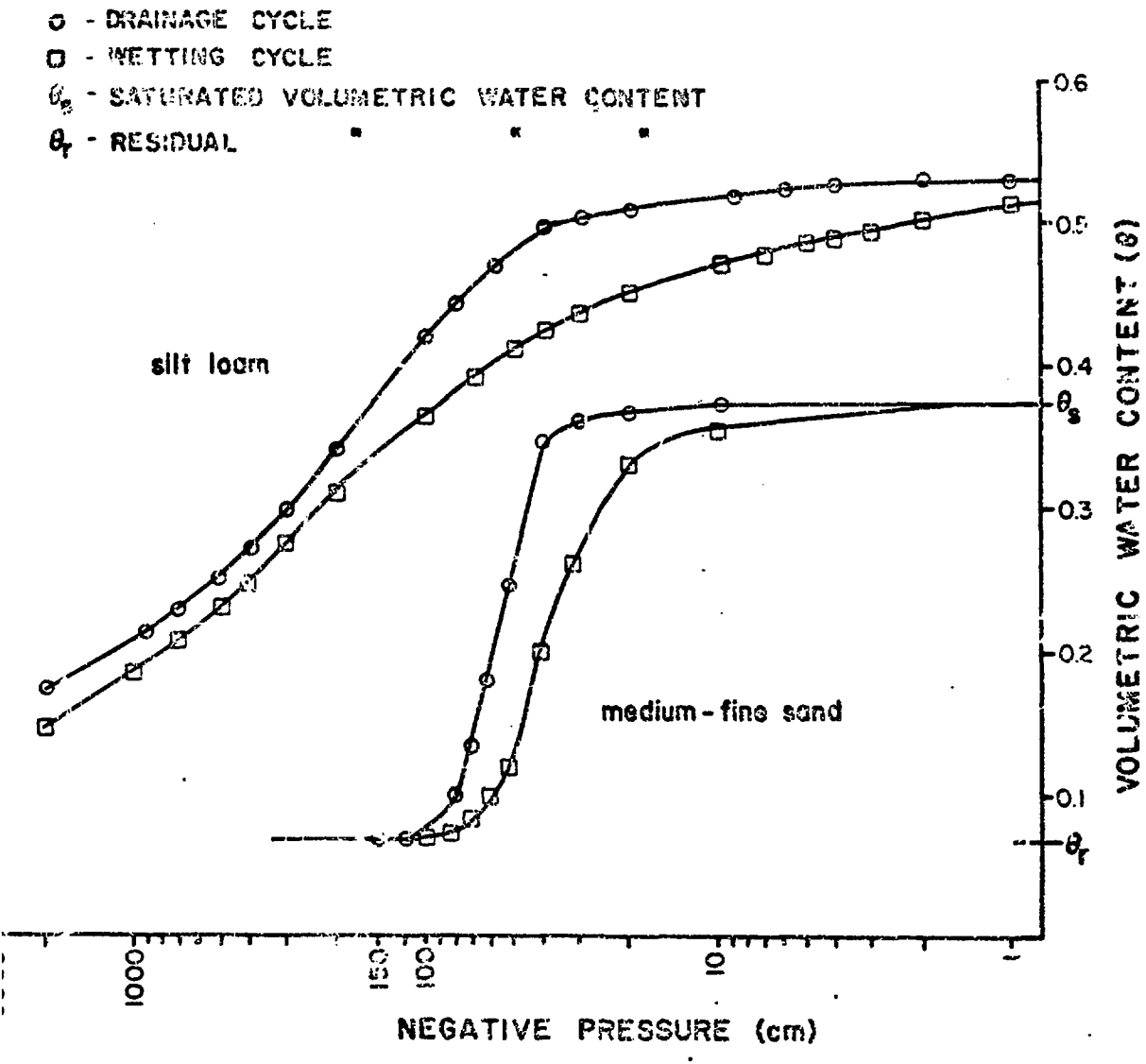

Figure 7(a). Wetting and draining curves for silt loam and medium-fine sand

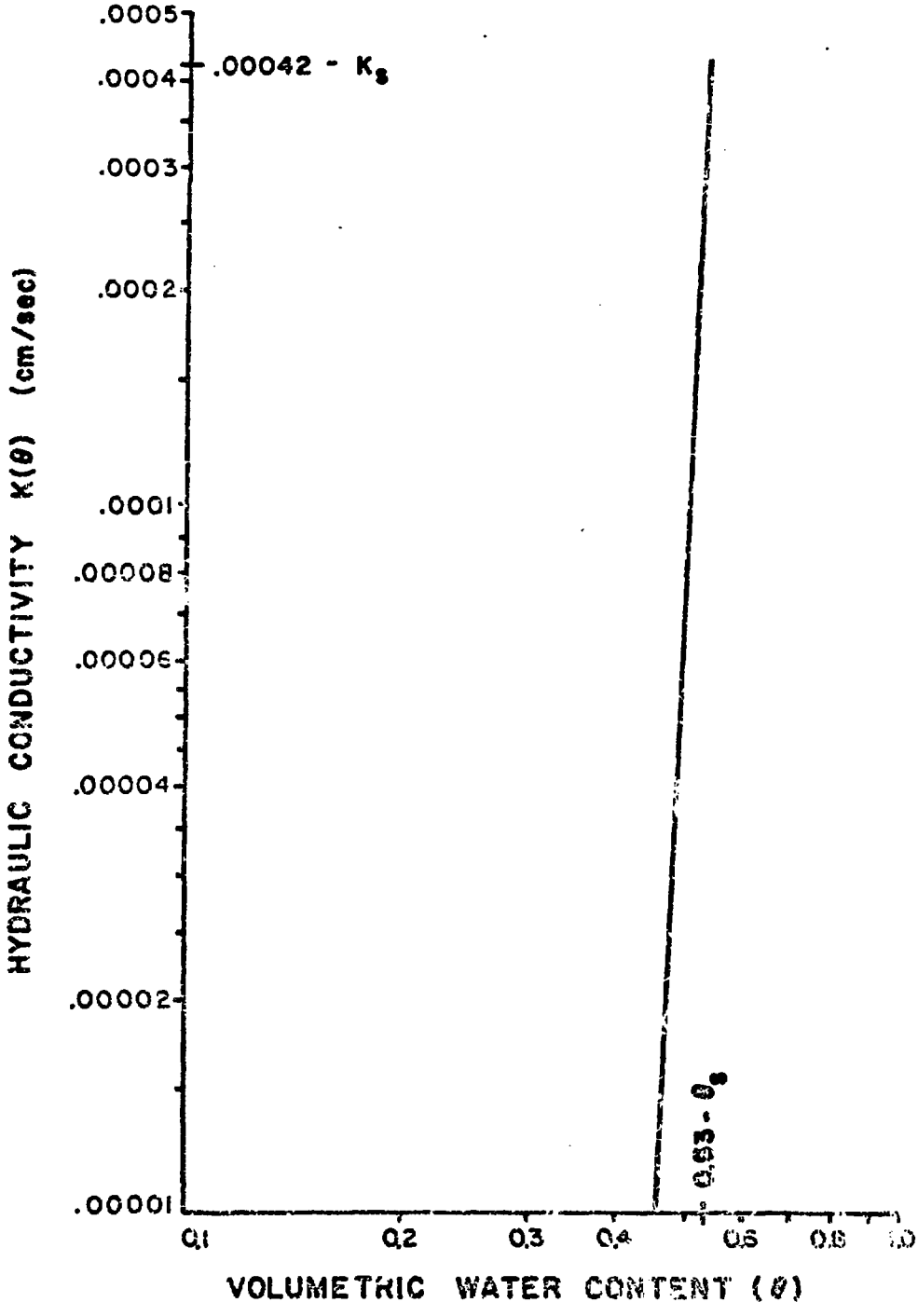

Figure 7(b). Hydraulic conductivity versus water content for silt loam

(a)

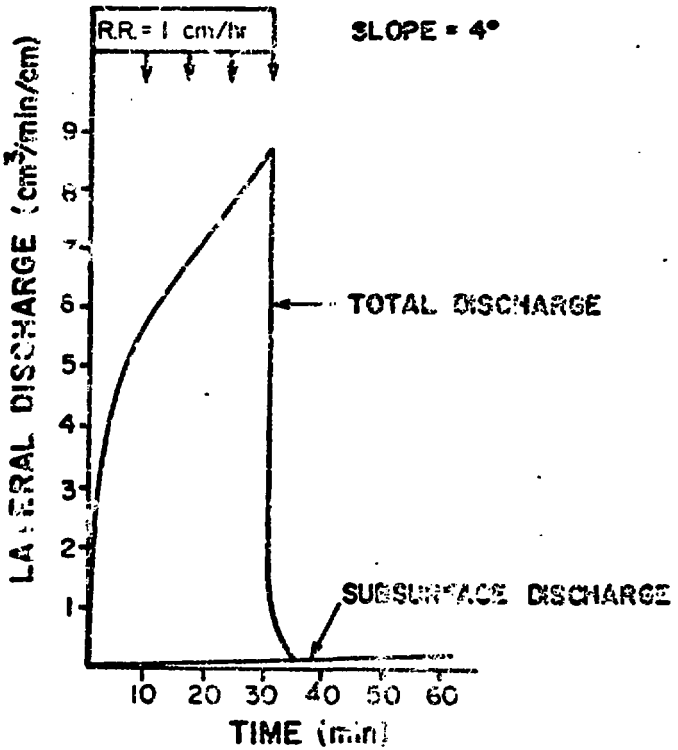

(b)

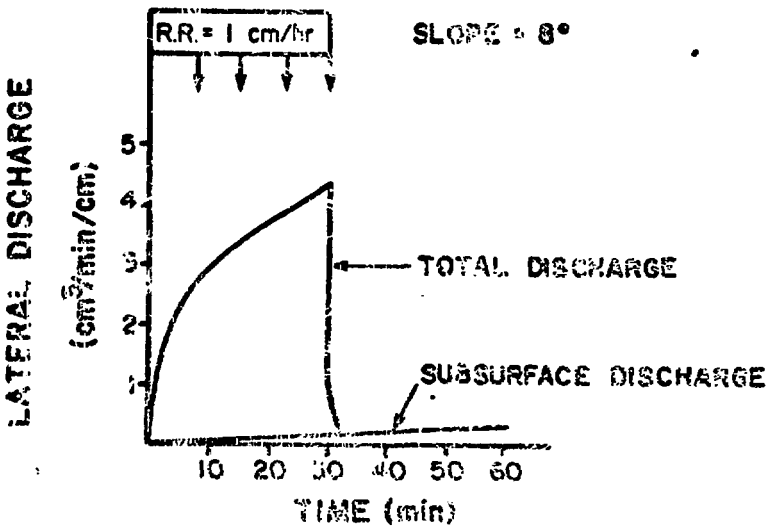

Figure 8. Hydrograph for silt loam: (a) surface slope = 4°
(b) surface slope = 8°